Analytical Science Advances

Chemistry Europe
European Chemical Societies Publishing

RESEARCH ARTICLE OPEN ACCESS

Gas Chromatography-Mass Spectrometry-Based Phytochemical Profiling and Bioactivity-Guided Fractionation of *Psidium guineense* Stem Extracts: In Vitro and In Silico Insights Into Antioxidant, Antidiabetic and Antibacterial Potentials

Md. Jahid Hossain[1] | Mst. Shagorika Shila[2] | Muhammad Rashedul Islam[1] | Jakir Ahmed Chowdhury[1]

[1]Department of Pharmaceutical Technology, Faculty of Pharmacy, University of Dhaka, Dhaka, Bangladesh | [2]Incepta Pharmaceuticals Ltd., Dhaka, Bangladesh

Correspondence: Md. Jahid Hossain (jahid-2015818069@pharmacy.du.ac.bd)

Received: 11 January 2026 | **Revised:** 13 March 2026 | **Accepted:** 18 March 2026

Keywords: DPPH scavenging | enzyme inhibition | molecular docking | Myrtaceae | traditional medicine | wild guava | α-amylase inhibition | α-glucosidase inhibition

ABSTRACT

Psidium guineense (Myrtaceae) is traditionally used for various medicinal purposes, although its stem remains underexplored. This study provides the first integrated phytochemical, pharmacological and computational evaluation of the stem extracts to elucidate their antioxidant, antidiabetic and antibacterial potential. The crude methanolic extract was fractionated with petroleum ether, dichloromethane, ethyl acetate and water. Preliminary phytochemical screening confirmed the presence of flavonoids, tannins, saponins, steroids, alkaloids, terpenoids and glycosides. Total phenolic and flavonoid contents were measured spectrophotometrically using the Folin–Ciocalteu reagent and the aluminium chloride colorimetric method, respectively. Antioxidant capacity was measured via 2,2-diphenyl-1-picrylhydrazyl (DPPH) assay, antidiabetic potential via α-amylase and α-glucosidase inhibition, and antibacterial activity via disc diffusion method. Gas Chromatography-Mass Spectrometry (GC-MS) profiling of the methanolic extract led to the identification of 28 phytoconstituents. Among all fractions, the dichloromethane fraction (DPG) exhibited the highest phenolic (247.94 ± 15.38 mg gallic acid equivalents/g) and flavonoid levels (510.27 ± 16.71 mg quercetin equivalents/g), along with superior DPPH radical scavenging capacity. DPG demonstrated scavenging activity (IC_{50} = 7.45 ± 0.87 μg/mL) comparable to ascorbic acid. In enzyme inhibition assays, DPG showed remarkable α-amylase and α-glucosidase inhibitory effects (IC_{50} = 22.28 ± 0.97 and 25.00 ± 2.01 μg/mL, respectively)—activities that surpass those reported for leaf extracts of related species. All fractions exhibited moderate, selective antibacterial activity against *B. subtilis* with zones of inhibition 7–16 mm. GC-MS profiling enabled tentative identification of compounds with reported antioxidant, antidiabetic and antimicrobial activities, supported by in silico docking showing strong predicted binding of selected tentatively identified constituents. These findings provide the first scientific investigation for the traditional use of *P. guineense* stem and highlight it as a previously unrecognized source of bioactive compounds warranting further isolation and characterization.

This is an open access article under the terms of the Creative Commons Attribution License, which permits use, distribution and reproduction in any medium, provided the original work is properly cited.

© 2026 The Author(s). *Analytical Science Advances* published by Wiley-VCH GmbH.

1 | Introduction

The escalating global burden of metabolic disorders, particularly diabetes mellitus, underscores an urgent need for safer therapeutic strategies [1, 2]. Diabetes, projected to affect 693 million people by 2045, is largely driven by postprandial hyperglycaemia, which is managed clinically using enzyme inhibitors such as acarbose [2]. However, these synthetic inhibitors are frequently associated with gastrointestinal side effects, prompting interest in plant-derived alternatives with potentially improved tolerability [3]. Diabetes is further complicated by oxidative stress, which contributes to disease progression and the development of comorbidities including neuropathy and cardiovascular disorders [4]. While synthetic antioxidants are available, their long-term safety remains a concern, driving the search for natural antioxidant sources [5]. Simultaneously, the rise of multidrug-resistant bacteria has compromised the efficacy of conventional antibiotics, creating a public health crisis that necessitates the discovery of new antimicrobial agents from diverse sources, including medicinal plants [6]. In this context, plants offer a unique advantage such as they produce complex mixtures of secondary metabolites that may simultaneously target multiple pathological processes, including hyperglycaemia, oxidative damage and microbial infection [7, 8].

The therapeutic effectiveness of phytomedicines is attributed to diverse secondary metabolites such as phenolics, flavonoids, alkaloids, tannins and terpenoids, known for their wide-ranging biological activities [9]. Within the rich biodiversity of medicinal flora, the genus *Psidium* (Myrtaceae) is notably significant [10]. *Psidium guajava* (common guava), for instance, has extensively been studied for its antidiabetic, antioxidant and antimicrobial properties [11]. *P. guineense* Swartz (Myrtaceae), commonly known as wild guava or Brazilian guava is a shrub or small tree native to tropical America, distributed from Mexico through Central America to northern Argentina and Brazil [12–14]. The species has been incorporated into traditional medicine systems across its native range and beyond. In Brazilian folk medicine, decoctions prepared from the leaves are widely used for the treatment of inflammatory conditions, while preparations of the roots and bark are employed to manage gastrointestinal disorders including diarrhoea and ulcers, and as a diuretic [12, 15].

However, a critical limitation exists in the current literature. Despite the ethnopharmacological relevance of *P. guineense*, all existing studies have focused exclusively on its aerial parts—specifically leaves and fruits. To the best of our knowledge, no integrated phytochemical and pharmacological evaluation of the stem has been reported. This represents a significant gap, as plant organs often accumulate distinct secondary metabolite profiles; compounds present in stems may differ qualitatively and quantitatively from those in leaves or fruits. Furthermore, the stem is typically discarded as agricultural waste during fruit harvesting [16, 17], and its valorization could transform an underutilized biomass into a valuable resource for drug discovery. To date, no integrated phytochemical or pharmacological investigation has been conducted on *P. guineense* stem, leaving its therapeutic potential entirely unknown.

To address this gap, an integrated experimental and computational workflow was employed. Bioactivity-guided fractionation of *P. guineense* stem extract was performed using solvents of increasing polarity, followed by phytochemical profiling (total phenolic and flavonoid contents) and in vitro evaluation of antioxidant, antidiabetic (α-amylase and α-glucosidase inhibition) and antibacterial activities. Individual constituents in active fractions were identified by GC-MS, and key compounds were further investigated through molecular docking and ADMET profiling to establish mechanistic insights and assess drug-likeness. This integrated approach was designed to identify bioactive constituents and provide molecular-level explanations, thereby addressing the knowledge gap regarding *P. guineense* stem and highlighting its potential for further investigation.

2 | Methods and Materials

2.1 | Chemicals and Reagents

All chemicals and solvents utilized were of analytical grade. Methanol, dichloromethane, n-hexane, ethyl acetate and distilled water for extraction and fractionation were obtained from Sigma-Aldrich (USA). Aluminium chloride, sodium carbonate, Folin–Ciocalteu reagent, dimethyl sulphoxide and DPPH were purchased from Merck (Germany). Reference standards, including gallic acid, quercetin and ascorbic acid, were sourced from Merck. Sodium phosphate buffer and p-nitrophenyl-α-D-glucopyranoside were employed in antidiabetic assays. Acarbose, used as the reference drug in α-amylase and α-glucosidase inhibition studies, was sourced from Square Pharmaceuticals Ltd. (Dhaka, Bangladesh). All microbiological media including Mueller-Hinton agar, nutrient broth and related materials were purchased from HiMedia Laboratories (India). The reference antibiotics kanamycin and fluconazole were obtained from Sigma-Aldrich for antimicrobial testing.

2.2 | Plant Material, Extraction and Fractionation

Stems of *P. guineense* Sw. were collected in February 2023 from the Comilla Hill tract, located in Cumilla District, Bangladesh, at geographic coordinates 23°27′30.5″ N latitude and 91°40′45.2″ E longitude (elevation approximately 45 m above sea level). The plants were growing in a mixed deciduous forest habitat along a hillside slope. Taxonomic authentication was performed by experts at the Bangladesh National Herbarium, Mirpur, Dhaka, where a voucher specimen (Accession No. DACB 32766) was deposited for future reference. Following collection, the stems were washed thoroughly with running tap water to remove adhering debris, cut into small pieces (approximately 2–3 cm length), and shade-dried at ambient temperature (25°C–28°C) for 7 days with adequate ventilation to prevent fungal growth. The dried stem pieces were then pulverized using a mechanical grinder to obtain a coarse powder, which was stored in airtight containers protected from light until extraction [18].

Approximately 500 g of the finely powdered *P. guineense* stem material were immersed in 3 L of methanol within opaque containers. This mixture was agitated for 7 days at room temperature to improve the comprehensive extraction of compounds into the solvent. Following maceration, the mixture was filtered using Whatman No. 1 paper to separate the plant residues, and

TABLE 1 | Phytochemical profiling of *P. guineense* stem extracts.

Test	MPG	PPG	DPG	EPG	WPG
Flavonoids	++	+	++	++	+
Anthraquinone	+++	+	+++	+++	++
Resins	+++	++	+++	+++	+++
Tannins	+++	+	+++	+++	+++
Glycosides	–	++	–	–	+
Phlobatannins	–	–	–	–	–
Saponins	+++	+	+++	+++	++
Steroids	+++	+	+++	++	+++
Alkaloids	+	–	+	+	–

Note: Abundance scale: +++ (high), ++ (moderate), + (low), – (absent).

the methanol was evaporated under reduced pressure to obtain a concentrated brown, viscous methanolic extract (MPG). A portion of the crude extract was retained for direct analysis, while the remaining bulk was subjected to a fractionation process using a modified Kupchan method [19].

For fractionation, the crude methanolic extract was sequentially partitioned using a series of solvents with increasing polarity. This technique allows for the separation of compounds based on their differential solubility in various solvents. The sequential partitioning yielded four distinct fractions: a petroleum ether fraction (PPG), a dichloromethane fraction (DPG), an ethyl acetate fraction (EPG) and an aqueous (water) fraction (WPG). This systematic fractionation enriches specific types of compounds in each fraction, making it easier to identify and characterize their individual bioactivities.

2.3 | Phytochemical and Bioactivity Assays

Preliminary phytochemical screening of all extracts (MPG, PPG, DPG, EPG, WPG) was conducted using standard qualitative tests for flavonoids, alkaloids, tannins, steroids, saponins, resins, anthraquinones, glycosides and phlobatannins [20]. Alkaloids were detected by Mayer's reagent (cream precipitate). Flavonoids were identified by Shinoda test (pink to red colour with Mg/HCl). Tannins were detected by ferric chloride test (blue-black or green-black precipitate). Saponins were identified by froth test (persistent foam). Steroids (reddish-brown interface) and terpenoids (yellow colour) were evaluated by Liebermann–Burchard test. Anthraquinones were detected by Borntrager's test (pink to violet in ammoniacal layer). Cardiac glycosides were identified by Keller–Kiliani test (brown ring). Resins were detected by acetic anhydride–sulphuric acid test (purple to violet colour). Phlobatannins were identified by boiling with HCl (red precipitate). Results were scored as strongly present (+++), moderately present (++), slightly present (+) or absent (−) and presented in Table 1.

DPPH radical scavenging capacity was evaluated according to a standard procedure [21]. Serial dilutions of extracts and ascorbic acid (6.25–400 μg/mL) were mixed with 0.1 mM methanolic DPPH solution. After 30 min incubation in the dark, absorbance was measured at 517 nm. Scavenging percentage was calculated as $([A_{control} - A_{sample}] / A_{control}) \times 100$. IC_{50} values were obtained by graphing inhibition percentages against sample concentrations. Total phenolic content (TPC) was measured using the Folin–Ciocalteu method with gallic acid as standard [22]. Briefly, 0.5 mL of each extract (50–400 μg/mL) was mixed with 2.5 mL of diluted Folin–Ciocalteu reagent, followed by 2 mL of 7.5% sodium carbonate. After 20 min incubation in the dark at 25°C, absorbance was measured at 756 nm. Results were expressed as mg gallic acid equivalents (GAE)/g. Total flavonoid content (TFC) was determined using the aluminium chloride colorimetric method with quercetin as standard [23]. Each extract was reacted with 2% $AlCl_3$ solution, incubated in the dark for 60 min, and absorbance was recorded at 415 nm. Results were expressed as mg quercetin equivalents (QCE)/g.

For α-amylase inhibition, 500 μL of each extract was pre-incubated with 500 μL of enzyme (0.5 mg/mL in phosphate buffer, pH 6.8) at 25°C for 10 min [24]. Then, 500 μL of 1% starch solution was added and incubated. The reaction was terminated by adding 1 mL of DNSA reagent, followed by boiling for 5 min. After dilution with 10 mL distilled water, absorbance was measured at 540 nm. For α-glucosidase inhibition, 50 μL of each extract was pre-incubated with 100 μL of enzyme solution (0.5 U/mL in phosphate buffer, pH 6.8) at 37°C for 10 min using an established protocol [25]. The reaction was initiated by adding 50 μL of 5 mM p-nitrophenyl-α-D-glucopyranoside and incubated for 30 min. The reaction was terminated with 100 μL of 0.1 M Na_2CO_3, and absorbance was measured at 405 nm. Acarbose served as the positive control in both enzyme assays. All tests were performed in triplicate, and IC_{50} values were calculated.

Antimicrobial activity was assessed using the disc diffusion method against *Bacillus subtilis, Escherichia coli, Salmonella typhi and Aspergillus niger*. Sterile 8-mm discs were impregnated with 10 μL of extract (500 μg/disc) or reference antibiotics (kanamycin 30 μg/disc for bacteria; fluconazole 30 μg/disc for fungus). Plates were incubated at 35°C for 24 h (bacteria) or 27°C for 24 h (fungus), and inhibition zones were measured and compared to controls [26].

GC-MS analysis of the methanolic extract was performed using a Shimadzu GCMS-QP2020 system with a DB-5MS column (30

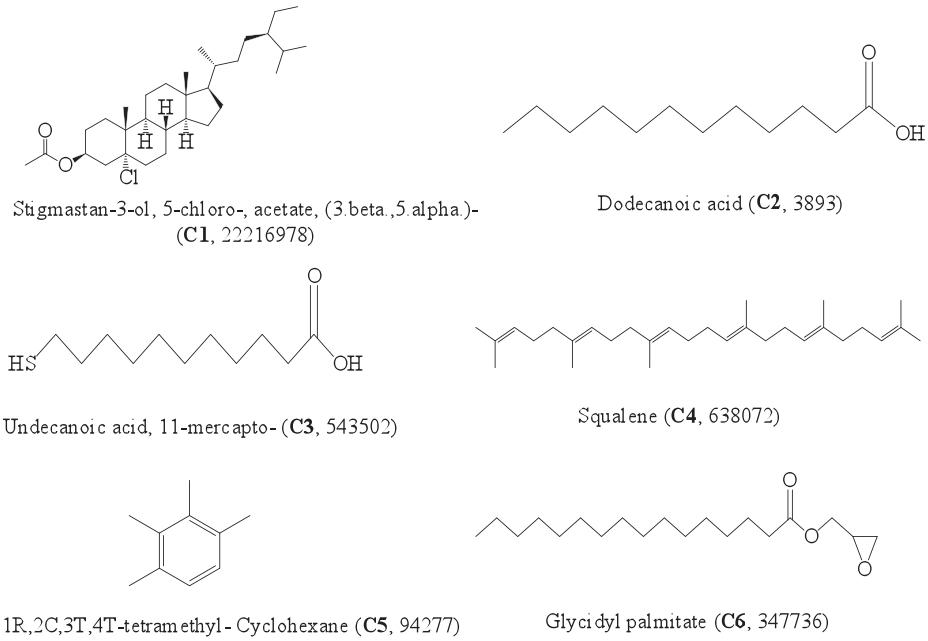


FIGURE 1 | Chemical structures of six major compounds from *P. guineense* stem selected for molecular docking. Compounds: C1 (stigmastan-3-ol, 5-chloro-, acetate), C2 (dodecanoic acid), C3 (undecanoic acid, 11-mercapto-), C4 (squalene), C5 (1R,2C,3T,4T-tetramethyl-cyclohexane), and C6 (glycidyl palmitate). PubChem CIDs are provided for each structure.

m × 0.25 mm i.d.) composed of a 5% diphenyl and 95% dimethyl polysiloxane stationary phase and helium as carrier gas. A 4 µL aliquot was injected in splitless mode at 220°C. Oven temperature was programmed from 80°C (2 min) to 150°C at 5°C/min, then to 280°C. Ionization was by electron impact at 70 eV. Mass spectra were recorded over a scan range of 40–650 m/z with a scan speed of 0.30 s per scan. Compounds were identified tentatively by comparing mass spectra with the NIST library (2008–2014), without confirmation using authentic reference standards or retention indices on columns of different polarities. While a similarity threshold of ≥ 85% was applied to increase confidence, definitive structural assignment would require additional validation using techniques such as co-injection with standards, retention index calculation or complementary spectroscopic methods.

2.4 | Computational Analysis

Six major compounds identified by GC-MS were selected for molecular docking based on their relative abundance and documented bioactivities activitieis in scientific literature. These compounds were: stigmastan-3-ol, 5-chloro-, acetate (C1), dodecanoic acid (C2), undecanoic acid, 11-mercapto- (C3), squalene (C4), 1R,2C,3T,4T-tetramethyl-cyclohexane (C5) and glycidyl palmitate (C6) (Figure 1). Their 3D structures were obtained from PubChem and minimized using Gaussian 09 W with the B3LYP/6-31G+(d,p) basis set.

Crystal structures of target proteins were obtained from the RCSB Protein Data Bank: human glutathione peroxidase 2 (2HE3) for DPPH radical scavenging capacity, human pancreatic α-amylase (4GQR) and human lysosomal alpha-glucosidase (5NN5) for antidiabetic activity and bacterial proteins from *B. subtilis* (1LNZ) and *S. typhimurium* (1TM2) for antibacterial activity. Proteins were prepared by removing water molecules and co-crystallized ligands using PyMOL, followed by energy minimization. Molecular docking was performed using AutoDock Vina within PyRx (v0.8). Grid boxes were centred on the active sites with dimensions optimized for each protein. The specific grid box sizes (x, y, z in Ångströms) were: 38.75 × 46.25 × 46.93 for 2HE3; 58.99 × 78.20 × 58.54 for 4GQR; 82.95 × 79.57 × 80.19 for 5NN5; 56.92 × 110.48 × 45.00 for 1LNZ; and 39.55 × 45.83 × 63.21 for 1TM2. Docking poses were ranked by binding affinity (kcal/mol), and the top poses were visualized using BIOVIA Discovery Studio to identify hydrogen bonds, hydrophobic interactions and other non-covalent contacts.

ADMET properties were predicted using the admetSAR online server. Biological activity spectra were predicted using the Prediction of Activity Spectra for Substances (PASS) tool [27]. Drug-likeness was evaluated using the SwissADME web server based on Lipinski, Ghose, Veber, Egan and Muegge filters, with bioavailability scores calculated accordingly [28, 29]. Key physicochemical parameters included molecular weight (MW, in Da), Wildman–Crippen log$P$ (WLOGP, a fragmental lipophilicity estimate), atom-additive log$P$ with corrections (XLOGP3, another lipophilicity predictor), molar refractivity (MR, in cm^3/mol, reflecting molecular volume and polarizability), and number of rotatable bonds (rotors, indicating molecular flexibility). The bioavailability score predicts the probability of oral bioavailability ≥ 10% in rats. Compounds violating multiple rules, common among larger natural products, may still possess therapeutic potential despite potentially reduced oral absorption.

2.5 | Statistical Evaluation

All tests involving quantitative measurements were performed three times, and results are denoted as mean values ± standard deviation (SD). Differences between groups were assessed using

TABLE 2 | Phytochemical content and bioactivity profile of *P. guineense* stem extracts.

Extracts of *P. guineense*	DPPH (IC_{50}) µg/mL	TPC (mg/g) equivalent of GA	TFC (mg/g) equivalent of QC	α-Amylase IC_{50} (µg/mL)	α-Glucosidase IC_{50} (µg/mL)
MPG	16.85 ± 1.29	149.29 ± 17.87	410.97 ± 8.23	46.77 ± 1.22	85.10 ± 2.00
PPG	26.48 ± 1.51	53.49 ± 13.32	116.90 ± 8.99	125.89 ± 1.09	102.00 ± 2.00
DPG	7.45 ± 0.87	247.94 ± 15.38	510.27 ± 16.71	22.28 ± 0.97	25.00 ± 2.01
EPG	11.31 ± 1.26	159.54 ± 15.27	441.84 ± 10.46	31.62 ± 1.08	59.33 ± 4.04
WPG	21.35 ± 1.26	135.45 ± 10.60	313.89 ± 12.19	43.65 ± 1.25	65.33 ± 2.52

Note: Data are mean ± SD, $n = 3$; *$p < 0.01$ are considered as the significance difference among groups.

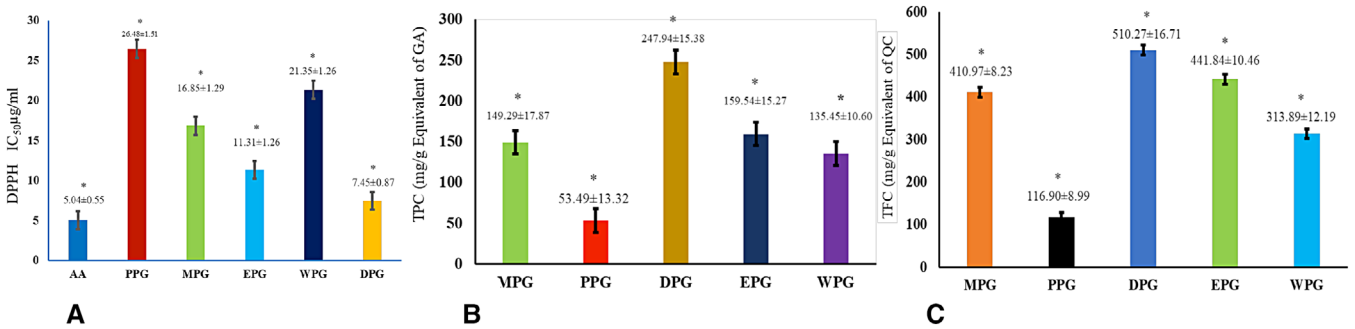


FIGURE 2 | Phytochemical profiling and antioxidant activity of *P. guineense* stem extracts. (A) DPPH radical scavenging activity expressed as IC_{50} values (µg/mL) compared to ascorbic acid. (B) Total phenolic content (mg GAE/g). (C) Total flavonoid content (mg QCE/g). Data represent mean ± SD ($n = 3$). *$p < 0.01$ compared among groups.

one-way ANOVA, with statistical significance set at $p < 0.01$. Statistical processing was performed using SPSS (version 29.0), while graphs were generated with GraphPad Prism (version 6.0).

3 | Results and Discussion

3.1 | Phytochemical Profiling and GC-MS Analysis

The preliminary phytochemical screening of *P. guineense* stem extracts confirmed the presence of diverse secondary metabolites including flavonoids, tannins, saponins, steroids, alkaloids and anthraquinones (Table 1). Flavonoids and tannins were consistently present across all fractions, while alkaloids were concentrated in the methanol (MPG), dichloromethane (DPG) and ethyl acetate (EPG) fractions but absent in the non-polar petroleum ether (PPG) and highly polar aqueous (WPG) fractions. This distribution pattern reflects the differential solubility of alkaloids in mid-polarity solvents [20]. Glycosides were detected only in the PPG and WPG fractions, indicating their preferential extraction in either non-polar or highly polar environments. These findings align with previous reports on *Psidium* species, where leaf extracts have shown similar phytochemical diversity [30, 31]. However, the present study provides the first documentation of such profiles specifically for the stem, suggesting potential organ-specific metabolite accumulation.

Quantitative analysis revealed significant variation in TPC and TFC across fractions (Table 2 and Figure 2). The dichloromethane fraction (DPG) exhibited the highest phenolic content (247.94 ± 15.38 mg GAE/g) and flavonoid content (510.27 ± 16.71 mg QCE/g), followed by EPG, MPG, WPG and PPG (see Tables S1 and S2, Figures S1–S4). This clear polarity-based gradient demonstrates that mid-polarity solvents (dichloromethane, ethyl acetate) are most effective at extracting phenolic and flavonoid compounds from the stem matrix. The TPC values obtained for the DPG fraction are substantially higher than those reported for *P. guineense* leaf extracts (54.34 ± 0.49 mg GAE/g) [32] and are comparable to or exceed values reported for other medicinally important *Psidium* species [33, 34]. This finding is particularly significant as it demonstrates that the stem—often discarded as agricultural waste—may harbour phenolic densities more prominent to the more commonly studied leaves. The high polyphenolic load in DPG provides a strong chemical basis for the bioactivity observed in subsequent assays, consistent with the well-established role of phenolics as primary antioxidant and enzyme inhibitory agents [21].

GC-MS profiling of the *P. guineense* methanolic extract revealed a complex chemical profile with 28 peaks detected in the chromatogram (Table 3). However, due to the complexity of the plant matrix, some peaks may represent co-eluting compounds rather than single, pure constituents. Therefore, the 28 peaks should be interpreted as chromatographic features, each potentially containing one or more phytoconstituents (see Figure S5). Tentative compound identification was performed on the major components within each peak where mass spectral deconvolution allowed for reasonable separation of co-eluting signals. The elution pattern depicted considerable diversity, with retention times ranging from 3.188 min (1,3-oxathiane, 5-*tert*-butyl-) to 38.421 min (stigmastan-3-ol, 5-chloro-, acetate, 3β,5α). Among

TABLE 3 | Tentative identification of major compounds from *Psidium guineense* methanolic stem extract by GC-MS analysis.

Peak no.	Retention time	Area (%)	Compound name	Molecular formula	Molecular weight
1	3.188	0.02	1,3-Oxathiane, 5-tert-butyl-	$CH_{16}OS$	160
2	3.620	2.10	Benzene, 1,3-dimethyl-	C_8H_{10}	106
10	15.090	0.88	5-Hydroxymethylfurfural	$C_6H_6O_3$	126
16	24.240	0.66	Neophytadiene	$C_{20}H_{38}$	278
20	**28.182**	**10.89**	**Dodecanoic acid**	**$C_{12}H_{24}O_2$**	**200**
21	**30.570**	**4.29**	**1r,2c,3t,4t-Tetramethyl-cyclohexane**	**$C_{10}H_{20}$**	**140**
25	**31.803**	**10.65**	**Undecanoic acid, 11-mercapto-**	**$C_{11}H_{22}O_2S$**	**218**
26	**34.726**	**3.90**	**Glycidyl palmitate**	**$C_{19}H_{36}O_3$**	**312**
27	**37.844**	**7.34**	**Squalene**	**$C_{30}H_{50}$**	**410**
28	**38.421**	**13.25**	**Stigmastan-3-ol, 5-chloro-, acetate (3β,5α)**	**$C_{31}H_{53}ClO_2$**	**492**

Note: Only compounds with area ≥ 0.66% (major peaks, > 50% total area) are shown; minor peaks omitted. Bold = selected for docking (abundance > 3%, documented bioactivity). Tentative identification by NIST library with similarity ≥ 85%; lower matches excluded.

all tentatively identified compounds, stigmastan-3-ol, 5-chloro-, acetate showed the highest relative abundance, contributing 13.25% of the total peak area, though GC-MS peak areas reflect detector response, not absolute concentration (see Table S3). Its identity as a chlorinated compound raises the possibility of an extraction artefact, as chlorinated natural products are uncommon in plants. This chlorinated stigmastanol derivative contrasts with typical leaf profiles of related species such as *P. guajava*, which are dominated by sesquiterpenes, caryophyllene oxide and flavonoid aglycones [35]. Other identified compounds included dodecanoic acid (10.89%), undecanoic acid, 11-mercapto- (10.65%), squalene (7.34%) and glycidyl palmitate (3.90%), all of which have established antimicrobial and antioxidant properties in the literature [36, 37]. The GC-MS profile thus confirms the presence of structurally diverse bioactive constituents ranging from oxygenated heterocycles to sterol derivatives, suggesting that these compounds may collectively contribute to the observed pharmacological properties of *P. guineense* stem. This chemical foundation, together with the high polyphenolic load in DPG, provides a strong basis for the bioactivity observed in subsequent assays, consistent with the well-established role of phenolics as primary antioxidant and enzyme inhibitory agents [21].

3.2 | Antioxidant Activity and Molecular Docking

All extracts exhibited concentration-dependent DPPH radical scavenging activity, with ascorbic acid (IC_{50} = 5.04 ± 0.55 μg/mL) serving as the positive control (Table 2). The DPG fraction demonstrated the most potent activity among plant extracts (IC_{50} = 7.45 ± 0.87 μg/mL), followed by EPG (11.31 ± 1.26 μg/mL), MPG (16.85 ± 1.29 μg/mL), WPG (21.35 ± 1.26 μg/mL) and PPG (26.48 ± 1.51 μg/mL) as presented in Table S4 and Figure S6. The superior activity of DPG correlates directly with its high phenolic and flavonoid content, consistent with the established hydrogen-donating and radical-stabilizing capabilities of these compounds [27]. The IC_{50} value of DPG is remarkably close to that of ascorbic acid and surpasses values reported for leaf extracts of related species, which typically range from 15–30 μg/mL [35, 36]. This positions the *P. guineense* stem, particularly its dichloromethane-soluble constituents, as a highly promising natural antioxidant source.

To establish a mechanistic rationale for this activity, molecular docking was performed against human glutathione peroxidase 2 (GPX2, PDB: 2HE3), a key enzyme in cellular antioxidant defence. Docking to GPX2 was performed to explore potential interactions with endogenous antioxidant defence enzymes rather than to directly model DPPH scavenging. Among the six major compounds identified by GC-MS (Table 4), squalene (C4) exhibited the strongest binding affinity (−6.8 kcal/mol), forming stable alkyl interactions with VAL21, VAL62 and pi-alkyl contacts with PHE26 (see Figures S7 and S8). This strong interaction is noteworthy, as squalene is a well-documented endogenous antioxidant, and its high abundance (7.34% of total peak area) in the extract provides a potential mechanistic link to the observed radical scavenging activity [38]. In addition, dodecanoic acid (C2) formed three conventional hydrogen bonds with key active site residues LEU101 (1.95 Å), LEU16 (2.57 Å) and ASP17 (2.35 Å) (see Table S5), further supporting the role of fatty acid derivatives in redox modulation, a phenomenon corroborated by studies on other plant oils [39]. These computational findings are consistent with the in vitro observations and identify specific compounds as potential contributors to the antioxidant potential of *P. guineense* stem.

3.3 | Antidiabetic Activity and Enzyme Inhibition

The antidiabetic potential of the extracts was evaluated through inhibition of α-amylase and α-glucosidase, key enzymes targeted in postprandial hyperglycaemia management [40]. For α-amylase inhibition (Figure 3), DPG again demonstrated the strongest activity (IC_{50} = 22.28 ± 0.97 μg/mL), second only to acarbose (13.13 ± 0.89 μg/mL), followed by EPG (31.62 ± 1.08 μg/mL), WPG (43.65 ± 1.25 μg/mL), MPG (46.77 ± 1.22 μg/mL) and PPG (125.89 ± 1.09 μg/mL) (see Figure S9 and Table S6). A similar trend was observed for α-glucosidase inhibition (Table 2),

TABLE 4 | Summary of molecular docking results for selected compounds against therapeutic targets.

Target (PDB)	Top compound	Binding affinity (kcal/mol)	Key interactions
Antioxidant (2HE3)	C4 (squalene)	−6.8	Alkyl: VAL21, VAL62; Pi-Alkyl: PHE26
α-Glucosidase (5NN5)	C1 (stigmastanol)	−7.2	H-bond: TYR360; Alkyl/Pi-Alkyl: multiple
α-Amylase (4GQR)	C1 (stigmastanol)	−9.0	Pi-Alkyl: VAL107, ILE51, TRP59
***B. subtilis* (1LNZ)**	C1 (stigmastanol)	−6.9	Alkyl: ARG252, LEU249; Pi-Alkyl: PHE166
***S. typhi* (1TM2)**	C1 (stigmastanol)	−8.8	Alkyl: LYS35, ALA222; Pi-Alkyl: TRP170

Note: Full docking data including all compounds and interaction distances are available in Table S7–S11.

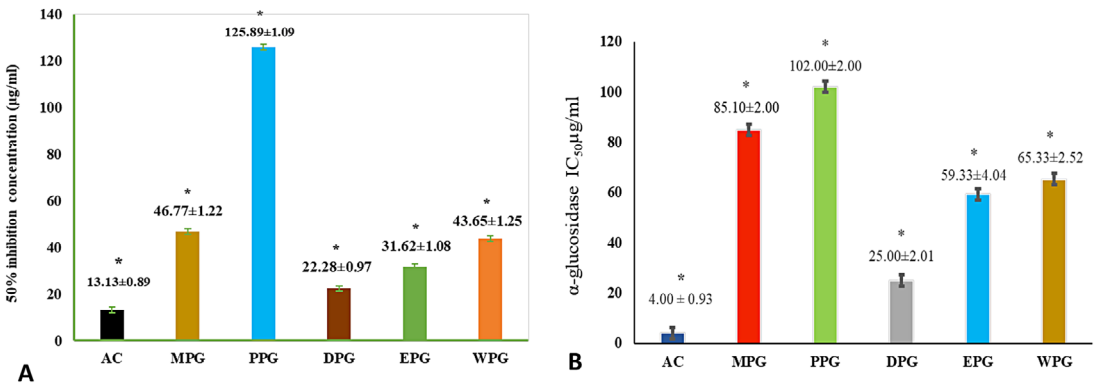


FIGURE 3 | Antidiabetic activity of *P. guineense* stem extracts via enzyme inhibition. (A) α-Amylase IC_{50} values (µg/mL). (B) α-Glucosidase IC_{50} values (µg/mL). Acarbose served as the standard inhibitor. Data represent mean ± SD ($n = 3$). *$p < 0.01$ compared among groups.

with DPG showing the highest activity among extracts (IC_{50} = 25.00 ± 2.01 µg/mL), followed by EPG (59.33 ± 4.04 µg/mL), WPG (65.33 ± 2.52 µg/mL), MPG (85.10 ± 2.00 µg/mL) and PPG (102.00 ± 2.00 µg/mL) (see Figure S10 and Table S7). The consistent superiority of DPG across both enzyme targets strongly implicates the mid-polarity phenolic and flavonoid constituents concentrated in this fraction as the primary active agents. These IC_{50} values compare favourably with those reported for *P. guajava* leaf extracts (20–50 µg/mL for α-amylase) [25], underscoring the previously unrecognized value of the stem. In vitro enzyme inhibition assays have inherent limitations: they use optimized conditions that do not replicate the gastrointestinal environment, and potency does not predict in vivo efficacy due to metabolism, protein binding and bioavailability. While the extract compares favourably with reported values for *P. guajava* leaf extracts [25], such comparisons require caution. These findings provide a rationale for animal model studies to assess true antidiabetic potential.

Molecular docking against human pancreatic α-amylase (4GQR) and human lysosomal alpha-glucosidase (5NN5) provided mechanistic validation (Table 4). Compound C1, a stigmastan-3-ol derivative and the most abundant compound in the extract (13.25% of total peak area), exhibited the strongest binding affinity to both α-amylase (−9.0 kcal/mol) and α-glucosidase (−7.2 kcal/mol) (see Figures S11–S14, Tables S8 and S9). Its predicted binding poses were stabilized by interactions including a hydrogen bond with TYR360 of α-glucosidase, a residue also involved in acarbose binding [41]. This computational finding suggests a potential competitive inhibition mechanism that could be similar to acarbose, though experimental validation (e.g., enzyme kinetics studies) is required to confirm the mechanism of action. The docking results align perfectly with the in vitro enzyme inhibition data, suggesting C1 as a priority for isolation and experimental validation and providing a coherent mechanistic explanation for the antidiabetic potential of *P. guineense* stem.

3.4 | Antibacterial Activity and Computational Validation

Antimicrobial testing revealed selective activity against the tested strains (Figure 4). All extracts were inactive against *E. coli* and *A. niger* at 500 µg/disc. However, activity was observed against

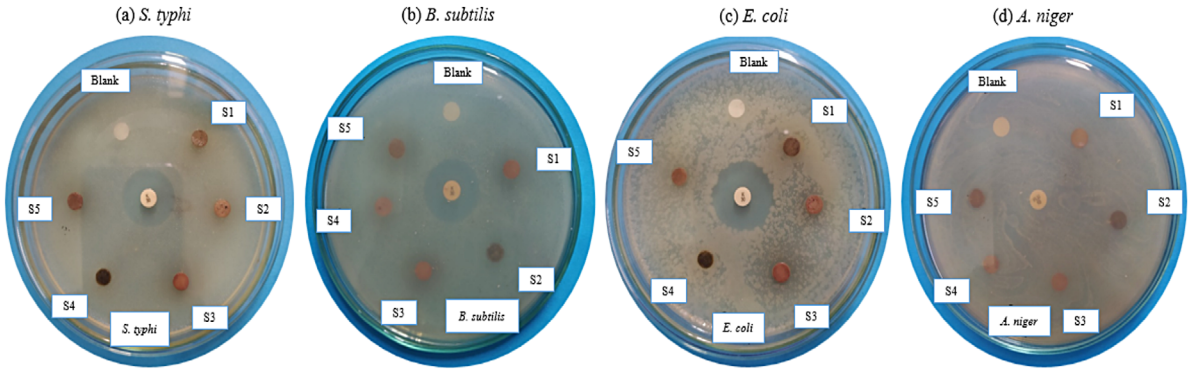


FIGURE 4 | Antimicrobial activity of *P. guineense* stem extracts. Disc diffusion assay with extracts (500 µg/disc) and standards (kanamycin 30 µg/disc; fluconazole 30 µg/disc). Values are mean zones of inhibition (mm) from triplicate experiments. DPG exhibited highest activity against *B. subtilis* (16 mm) and *S. typhi* (13 mm). (-) = no inhibition. All extracts inactive against *E. coli* and *A. niger*.

TABLE 5 | Antimicrobial effects of *Psidium guineense* stem extracts expressed as zones of inhibition in millimetres.

Extracts/standard	Zone of inhibition (mm)			
	Bacteria			Fungus
	E. coli **(−ve)**	***S. typhi*** **(−ve)**	***B. subtilis*** **(+ve)**	***A. niger***
Blank	—	—	—	—
Fluconazole (30 µg/disc)	—	—	—	12
Kanamycin (30 µg/disc)	23	21	22	—
MPG (500 µg/disc)	—	—	13	—
PPG (500 µg/disc)	—	—	07	—
DPG (500 µg/disc)	—	13	16	—
EPG (500 µg/disc)	—	—	07	—
WPG (500 µg/disc)	—	12	14	—

B. subtilis (Gram-positive) and *S. typhi* (Gram-negative). Against *B. subtilis*, DPG produced the largest inhibition zone (16 mm), followed by WPG (14 mm), MPG (13 mm) and PPG/EPG (7 mm each). Against *S. typhi*, DPG again showed the highest activity (13 mm), followed by WPG (12 mm). Kanamycin (30 µg/disc) produced zones of 22 mm (*B. subtilis*) and 21 mm (*S. typhi*), while fluconazole produced a 12 mm zone against *A. niger* (Table 5). The preferential activity against Gram-positive *B. subtilis* is consistent with the known susceptibility of these bacteria to phenolic compounds, which more readily penetrate the less complex Gram-positive cell wall [42]. The moderate activity against Gram-negative *S. typhi* suggests that some constituents may also target mechanisms beyond membrane disruption. This selective pattern differs from broader-spectrum activity reported for some *P. guajava* leaf extracts [13, 43], potentially reflecting the distinct phytochemical profile of the stem.

Molecular docking against bacterial targets provided mechanistic insights (Table 4). For *B. subtilis* (SPO0B-associated GTP-binding protein, Obg, PDB: 1LNZ), C1 again exhibited the strongest binding (−6.9 kcal/mol), forming alkyl and pi–alkyl interactions with ARG252, LEU249 and PHE166. C6, C3 and C2 formed hydrogen bonds with active site residues including SER168, LEU249, GLU250 and GLY251 (See Figures S15 and S16, Table S10). For *S. typhi* (LsrB AI-2 receptor, PDB: 1TM2), C1 showed the highest affinity (-8.8 kcal/mol) with extensive alkyl and pi-alkyl contacts. C6 formed a critical hydrogen bond with GLN167 (2.01 Å), while C2 and C3 both hydrogen-bonded with ALA222 (see Figures S17 and S18, Table S11). These targets are involved in bacterial stress adaptation (*B. subtilis*) and quorum sensing (*S. typhi*), processes indirectly linked to bacterial survival and virulence [44]. The computational evidence thus points to specific, target-based mechanisms rather than non-specific membrane disruption, explaining the observed selective antibacterial effects despite moderate inhibition zones.

To assess the therapeutic potential of the tentatively identified compounds, PASS prediction and drug-likeness profiling were performed (Table 6). PASS analysis predicted a broad spectrum of activities, including antioxidant (Pa 0.152-0.657), anti-inflammatory (C5: 0.713), antibacterial (C4: 0.397) and hepatoprotective (C1: 0.667) effects, expanding the potential therapeutic applications of *P. guineense* beyond the tested parameters (see Table S12). Drug-likeness evaluation revealed that compounds C2 (dodecanoic acid) and C3 (undecanoic acid, 11-mercapto-) exhibited excellent predicted oral bioavailability, complying with

TABLE 6 | In silico prediction of biological activities and drug-likeness parameters for selected compounds from *P. guineense* stem.

Compound	PASS prediction (Pa)				Drug-likeness parameters							
	Antioxidant	Anti-inflammatory	Hepato protectant	Anti bacterial	Lipinski	Ghose	Veber	Egan	Muegge	Bioavailability score	HBD	HBA
C1	0.521	0.505	0.667	0.324	Y (1)	N (4)	Y	N (1)	N (1)	0.55	0	2
C2	**0.222**	**0.515**	**0.491**	**0.300**	**Y**	**Y**	**Y**	**Y**	**Y**	**0.85**	**1**	**2**
C3	**0.282**	**0.433**	**0.587**	**0.217**	**Y**	**Y**	**Y**	**Y**	**Y**	**0.85**	**1**	**2**
C4	0.657	0.701	0.457	0.397	Y (1)	N (3)	N (1)	N (1)	N (2)	0.55	0	0
C5	0.152	0.713	0.323	0.280	Y (1)	N (1)	Y	Y	N (2)	0.55	0	0
C6	0.213	0.404	0.348	0.131	Y	Y	N (1)	Y	N (2)	0.55	0	3

Note: Egan (log$P \leq 5.88$, TPSA ≤ 131.6 Å^2); Ghose (MW 160–480, log$P$ −0.4 to 5.6, MR 40–130, atoms 20–70); HBD/HBA, hydrogen bond donors/acceptors; Muegge (MW 200–600, log$P$ −2 to 5, TPSA ≤ 150, rotatable bonds ≤ 15, HBD ≤ 5, HBA ≤ 10, ring count ≤ 7, carbon > 4, heteroatom > 1). Compliance: Y = passes, N = violates (violations in parentheses). Bold values indicate excellent predicted oral bioavailability (score ≥ 0.85); Pa, probability of activity (PASS prediction). Drug-likeness evaluated using five rule sets: Lipinski (MW ≤ 500, log$P \leq 5$, HBD ≤ 5, HBA ≤ 10); Veber (rotatable bonds ≤ 10, TPSA ≤ 140 Å^2).

all Lipinski, Ghose, Veber, Egan and Muegge rules and achieving a bioavailability score of 0.85, as presented in Table S13 [45]. In contrast, the docking candidates with higher predicted binding affinities (C1, C4, C5 and C6) violated multiple parameters, resulting in lower bioavailability scores (0.55). This highlights a common challenge in natural product drug discovery: compounds with strong target affinity may require structural modification to optimize pharmacokinetic properties. It also underscores the value of the whole extract or standardized fraction (DPG), where synergistic combinations of compounds like C1 (high affinity) and C2 (high bioavailability) may offer an effective therapeutic complex balancing potency with absorption.

Pharmacokinetic profiling further supported these observations, revealing that C1 and C4 exhibited high human intestinal absorption (HIA ≥ 0.988) and blood–brain barrier penetration (BBB ≥ 0.900), while C2 and C3 demonstrated favourable toxicity profiles with no P-glycoprotein inhibition and lower hepatotoxicity risk (see Table S14). Notably, C1 and C4 were predicted as P-glycoprotein inhibitors, which may impact their systemic disposition, whereas all compounds fell within acute toxicity Categories III–IV, indicating relatively safe profiles. This integrated analysis highlights the need to balance target affinity with favourable absorption, distribution, metabolism, excretion and toxicity (ADMET) properties in selecting lead candidates for further development.

4 | Conclusion

This integrated study provides preliminary evidence supporting traditional uses of *P. guineense* stem, suggesting it as a potential source of bioactive compounds warranting further investigation. The systematic solvent fractionation proved crucial, revealing that the dichloromethane-soluble constituents (DPG) are the most pharmacologically active, correlating with its high phenolic and flavonoid content. The extract's significant radical scavenging and reducing power, coupled with potent in vitro inhibition of α-amylase and α-glucosidase, provides evidence for its traditional use in managing oxidative stress and diabetes. This anti-hyperglycaemic potential is particularly notable, with the DPG fraction exhibiting enzyme inhibitory activity comparable to reports on the leaves of the well-studied *P. guajava*.

Furthermore, the selective antibacterial activity against *B. subtilis*, supported by tentative GC-MS identification of 28 phytoconstituents and in silico docking to key bacterial enzymes, underscores the multi-target therapeutic capacity of this plant material. Computational analyses tentatively identified stigmastanol derivative (C1) and squalene (C4) as compounds of interest based on their predicted binding affinities to diabetic and antioxidant targets, respectively. However, these compound identities require confirmation through isolation and spectroscopic characterization (e.g., NMR), and their proposed contributions to bioactivity require experimental validation using purified compounds. Predictive ADMET and drug-likeness profiling offered a potential for further investigation in drug discovery pipelines, highlighting dodecanoic acid (C2) as a compound with an excellent bioavailability profile.

However, the in vitro nature of this study represents a significant limitation, and the findings should be interpreted as preliminary evidence rather than definitive proof of therapeutic efficacy. The observed bioactivities and computational predictions require validation through in vivo studies to assess true pharmacological potential, bioavailability, metabolism and toxicity in complex biological systems. In addition, the specific compounds responsible for the observed activities remain to be isolated and characterized through bioassay-guided fractionation, followed by confirmation of their individual and synergistic effects.

In conclusion, this work successfully transitions *P. guineense* stem from an underexplored agricultural by-product to a validated source of multi-target bioactive agents. The findings provide preliminary support for its traditional applications and support the need for further investigation. Future studies should aim at the bioassay-guided isolation and characterization of the specific compounds, particularly Stigmastanol, to confirm their individual bioactivities and mechanisms, followed by preclinical in vivo studies to assess safety and efficacy. This study provides a strong

basis for the development of standardized phytopharmaceuticals or nutraceuticals derived from *P. guineense* stem, contributing to sustainable drug discovery from natural biodiversity while valorizing an underutilized agricultural by-product.

Author Contributions

Md. Jahid Hossain: supervision, investigation, formal analysis, conceptualization, project administration, writing – original draft. **Mst. Shagorika Shila**: writing – review and editing, writing – original draft, validation, formal analysis, visualization, methodology. **Muhammad Rashedul Islam**: investigation, conceptualization. **Jakir Ahmed Chowdhury**: conceptualization.

Acknowledgements

The authors sincerely acknowledge the Department of Pharmacy at East West University, Bangladesh, for providing research facilities and logistical support. Generative AI tools were used solely to enhance language and readability. All content was subsequently reviewed and edited by the authors, who take full responsibility for the final version.

Ethics Statement

The authors have nothing to report.

Consent

The authors have nothing to report.

Conflicts of Interest

The authors declare no conflicts of interest.

Data Availability Statement

All relevant data generated and analysed during this study are included in this published article and its Supporting Information files. The Supporting Information contains detailed docking interaction tables, raw GC-MS chromatograms and 2D interaction diagrams for all protein–ligand complexes. Mass spectral data and molecular docking output files (PDBQT formats) are available from the corresponding author upon reasonable request.

References

1. N. Wang and C. Zhang, "Oxidative Stress: A Culprit in the Progression of Diabetic Kidney Disease," *Antioxidants* 13, no. 4 (2024): 455, https://doi.org/10.3390/antiox13040455..

2. M. Tumurkhuu, S. A. Bhat, M. Z. Hossain, et al., "Cellular and Molecular Mechanisms in Metabolic Disorders: Role of Inflammation and Oxidative Stress," *Frontiers in Pharmacology* 16 (2025): 1580553, https://doi.org/10.3389/fphar.2025.1580553.

3. M. F. Mahomoodally, D. Lobine, M. C. Picot-Allain, et al., "Conventional and Non-Conventional Targets of Natural Products in the Management of Diabetes Mellitus and Associated Complications," *Current Medicinal Chemistry* 28, no. 23 (2021): 4638–4669, https://doi.org/10.2174/0929867327666201102120120.

4. K. Jomova, R. Raptova, S. Y. Alomar, et al., "Reactive Oxygen Species, Toxicity, Oxidative Stress, and Antioxidants: Chronic Diseases and Aging," *Archives of Toxicology* 97, no. 10 (2023): 2499–2574, https://doi.org/10.1007/s00204-023-03562-9.

5. M. Sharifi-Rad, N. V. Anil Kumar, and P. Zucca, "Lifestyle, Oxidative Stress, and Antioxidants: Back and Forth in the Pathophysiology of Chronic Diseases," *Frontiers in Physiology* 11 (2020): 552535, https://doi.org/10.3389/fphys.2020.00694.

6. R. D. Süssmuth, "Fighting Antimicrobial Resistance: Innovative Drugs in Discovery and Design," *Angewandte Chemie International Edition* 64 (2025): e202414325, https://doi.org/10.1002/anie.202414325.

7. R. Latif and T. Nawaz, "Medicinal Plants and Human Health: A Comprehensive Review of Bioactive Compounds, Therapeutic Effects, and Applications," *Phytochemistry Reviews* 25 (2025): 1–44, https://doi.org/10.1007/s11101-025-10194-7.

8. M. I. Jahan Oni, "Botanical Sources, Pharmacokinetics, and Therapeutic Efficacy of Palmatine and Its Derivatives in the Management of Cancer: A Comprehensive Mechanistic Analysis," *Journal of Food Biochemistry* 2024 (2024): 8843855, https://doi.org/10.1155/2024/8843855.

9. T. M. Al-Raddadi, S. O. Bahaffi, and L. A. Alk-hateeb, "Phytochemical Analysis and Compound Profiling of *Boerhavia elegans* Stem Extract Using GC–MS," *Analytical Science Advances* 6 (2025): e70011, https://doi.org/10.1002/ansa.70011..

10. J. G. F. Macedo, M. de Oliveira Santos, C. D. F. A. Nonato, et al., "Chemical Composition, Antioxidant, Antibacterial and Modulating Activity of the Essential Oil of *Psidium* L. Species (Myrtaceae Juss.)," *Biocatalysis and Agricultural Biotechnology* 42 (2022): 102363, https://doi.org/10.1016/j.bcab.2022.102363.

11. E. Butt, A. B. Altemimi, A. Younas, et al., "Guava (*Psidium guajava*): A Brief Overview of Its Therapeutic and Health Potential," *Food Chemistry: X* 31 (2025): 103027, https://doi.org/10.1016/j.fochx.2025.103027.

12. J. E. Vielma-Puente, E. Santos-Ordóñez, X. Cornejo, et al., "DNA Barcode, Chemical Analysis, and Antioxidant Activity of *Psidium guineense* From Ecuador," *PLoS ONE* 20, no. 3 (2025): e0319524, https://doi.org/10.1371/journal.pone.0319524.

13. K. F. do Nascimento, F. M. F. Moreira, J. A. Santos, et al., "Antioxidant, Anti-Inflammatory, Antiproliferative and Antimycobacterial Activities of the Essential Oil of *Psidium guineense* Sw. and Spathulenol," *Journal of Ethnopharmacology* 210 (2018): 351–358, https://doi.org/10.1016/j.jep.2017.08.030.

14. T. G. Fernandes, A. R. C. de Mesquita, K. P. Randau, et al., "In Vitro Synergistic Effect of *Psidium guineense* (Swartz) in Combination With Antimicrobial Agents Against Methicillin-Resistant *Staphylococcus aureus* Strains," *Scientific World Journal* 2012, no. 1 (2012): 158237, https://doi.org/10.1100/2012/158237.

15. K. F. do Nascimento, C. A. L. Kassuya, M. R. P. Cabral, et al., "Chemical Analysis and Antioxidant, Anti-Inflammatory and Toxicological Evaluations of the Hydromethanolic Extract of *Psidium guineense* Swartz Leaves," *Journal of Ethnopharmacology* 281 (2021): 114492, https://doi.org/10.1016/j.jep.2021.114492.

16. T. R. Fasola, G. K. Oloyede, and B. S. Aponjolosun, "Chemical Composition, Toxicity and Antioxidant Activities of Essential Oils of Stem Bark of Nigerian Species of Guava (*Psidium guajava* Linn.)," *EXCLI Journal* 10 (2011): 34–43..

17. H. T. Manekeng , A. T. Mbaveng, S. A. Ntyam Mendo, et al., "Evaluation of Acute and Subacute Toxicities of *Psidium guajava* Methanolic Bark Extract: A Botanical With In Vitro Antiproliferative Potential," *Evidence-Based Complementary and Alternative Medicine* 11 (2019): 8306986, https://doi.org/10.1155/2019/8306986.

18. M. M. Nadzir, F. N. Idris, and C. J. Yi, "Phenolic Compounds and Antioxidant Activities of Macerated *Alpinia galanga* Stems and Leaves," *ASEAN Engineering Journal* 10, no. 1 (2020): 40–48, https://doi.org/10.11113/AEJ.V10.15537.

19. S. Banfi, E. Caruso, V. Orlandi, et al., "Antibacterial Activity of Leaf Extracts From *Combretum micranthum* and *Guiera senegalensis* (Combretaceae)," *Research Journal of Microbiology* 9, no. 2 (2014): 66, https://doi.org/10.3923/jm.2014.66.81.

20. M. N. Mousumy, F. Uddin, and K. Saha, "Phytochemical Screening of Plant Extracts and GC-MS Analysis of the n-Hexane Soluble Part of the Crude Chloroform Extract of Seed Pods of *Cassia fistula* Growing

in Bangladesh," *Journal of Pharmacognosy and Phytochemistry* 14, no. 1 (2025): 220–225, https://doi.org/10.22271/phyto.2025.v14.i1c.15238.

21. G. Aquino, E. M. Sommella, E. Salviati, et al., "Advancing Profiling of Secondary Antioxidant Metabolites in Allium Cepa PDO Leaf Extract: Online Comprehensive Two-Dimensional Liquid Chromatography With High-Resolution Mass Spectrometry and Pre-Column DPPH Assay," *Journal of Chromatography A* 1749 (2025): 465877, https://doi.org/10.1016/j.chroma.2025.465877.

22. A. S. Farha, M. A. Samadd, N. Akter, et al., "Integrated Phytochemical and Pharmacological Assessment of *Uraria rufescens* Leaves: Insights Into Its Antioxidant, Thrombolytic and CNS Activities," *Analytical Science Advances* 6, no. 2 (2025): e70049, https://doi.org/10.1002/ansa.70049.

23. Y. K. Unda and E. S. Wulo, "Analysis of Absorbance Value of Flavonoid Level in Brotowali Stem Extract Using UV-Vis Spectrophotometer," *Jurnal Penelitian Pendidikan IPA* 11, no. 6 (2025): 284–289, https://doi.org/10.29303/jppipa.v11i6.10066.

24. M. N. Beidokhti, H. M. Eid, M. L. Villavicencio, et al., "Evaluation of the Antidiabetic Potential of *Psidium guajava* L. (Myrtaceae)," *Journal of Ethnopharmacology* 257 (2020): 112877, https://doi.org/10.1016/j.jep.2020.112877.

25. M. Daou, N. A. Elnaker, M. A. Ochsenkühn, et al., "In Vitro α-Glucosidase Inhibitory Activity of *Tamarix nilotica* Shoot Extracts and Fractions," *PLoS ONE* 17, no. 3 (2022): e0264969, https://doi.org/10.1371/journal.pone.0264969.

26. Z. Yang, L. Li, C. H. Chen, et al., "Chemical Composition and Antibacterial Activity of 12 Medicinal Plant Ethyl Acetate Extracts Using LC-MS Feature-Based Molecular Networking," *Phytochemical Analysis* 33, no. 3 (2022): 473–489, https://doi.org/10.1002/pca.3103.

27. M. R. Hossain, M. Uzzaman, K. Fatema, et al., "DFT and In Silico Study of Printing Ink Toxicity on Human Health," *Discover Chemistry* 2, no. 1 (2025): 216, https://doi.org/10.1007/s44371-025-00296-8.

28. Y. Saristiana, F. Prasetyawan, M. B. Abd Kadir, et al., "Prediction of Activity Spectra for Substances (PASS) From Mangiferin Bioactive Mango," *Multidisciplinary Perspectives in Science and Technology* 1, no. 1 (2025): 53–66, https://doi.org/10.55927/mpst.v1i4.4.

29. I. Ahmad, H. Khan, and G. Serdaroğlu, "Physicochemical Properties, Drug Likeness, ADMET, DFT Studies, and In Vitro Antioxidant Activity of Oxindole Derivatives," *Computational Biology and Chemistry* 104 (2023): 107861, https://doi.org/10.1016/j.compbiolchem.2023.107861..

30. H. D. Huynh, P. Nargotra, H. M. D. Wang, et al., "Bioactive Compounds From Guava Leaves (*Psidium guajava* L.)," *Molecules* 30, no. 6 (2025): 1278, https://doi.org/10.3390/molecules30061278.

31. Y. Emam, R. M. Abdou, I. Y. Younis, et al., "Metabolomics in Guava: A Comprehensive Review of Quality, Agricultural Traits, Composition, and Nutraceutical Applications of *Psidium guajava* Fruits and Byproducts," *Phytochemistry Reviews* 24, no. 1 (2025): 1–23, https://doi.org/10.1007/s11101-025-10153-2.

32. J. E. Vielma-Puente, E. Santos-Ordóñez, X. Cornejo, et al., "DNA Barcode, Chemical Analysis, and Antioxidant Activity of *Psidium guineense* From Ecuador," *PLoS ONE* 20, no. 3 (2025): e0319524, https://doi.org/10.1371/journal.pone.0319524.

33. F. J. Álvarez-Martínez, E. Barrajón-Catalán, J. A. Encinar, et al., "Antimicrobial Capacity of Plant Polyphenols Against Gram-Positive Bacteria: A Comprehensive Review," *Current Medicinal Chemistry* 27, no. 15 (2020): 2576–2606, https://doi.org/10.2174/0929867325666181008115650.

34. A. Turay, M. D. Kamara, E. B. S. Conteh, et al., "Phytochemical Screening and Antimicrobial Studies of *Psidium guajava* (Guava) Plant," *International Journal of Pharmacognosy and Pharmaceutical Sciences* 7, no. 1 (2025): 1–7, https://doi.org/10.33545/27067009.2025.v7.i1a.168.

35. P. C. da Silva Santos, R. Gallo, E. R. Lima Nonato, et al., "*Psidium cattleyanum* Sabine: A Bibliometric Approach Focused on Its Bioactive Properties and Applications," *Forests, Trees and Livelihoods* 33, no. 3 (2024): 207–230, https://doi.org/10.1080/14728028.2024.2343919.

36. M. A. Lozano-Grande, S. Gorinstein, E. Espitia-Rangel, et al., "Plant Sources, Extraction Methods, and Uses of Squalene," *International Journal of Agronomy* 2018, no. 1 (2018): 1829160, https://doi.org/10.1155/2018/1829160.

37. K. Renugadevi, C. V. Nachiyar, and M. Zaveri, "Bioactivity of Dodecanoic Acid Extracted From Geitlerinema sp. TRV57," *Indian Journal of Pharmaceutical Education & Research* 55, no. 1 (2021): 224–231, https://doi.org/10.5530/ijper.55.1.25.

38. R. Patel, G. Singh, K. Kajal, et al., "Exploring FabH Inhibitors for Antimicrobial Therapy: Medicinal Chemistry, Synthetic Approaches, and SAR Evaluation," *Molecular Diversity* 29 (2025): 1–51, https://doi.org/10.1007/s11030-025-11383-4.

39. M. T. Frangipane, S. Garzoli, R. Massantini, et al., "Characterizing the Antioxidant Activity, Fatty Acids, and Volatile Compounds of Extra virgin Olive Oils," *European Journal of Lipid Science and Technology* 127 (2025): e70014, https://doi.org/10.1002/ejlt.70014.

40. M. Ni, X. Hu, D. Gong, and G. Zhang, "Inhibitory Mechanism of Vitexin on α-Glucosidase," *Food Hydrocolloids* 105 (2020): 105824, https://doi.org/10.1155/2021/6641128.

41. K. Ratananikom, P. Piyaviriyakul, and S. Suttisansanee, "In Vitro Evaluation of α-Glucosidase and α-Amylase Inhibitory Activities of Selected Plant Extracts With Antidiabetic Potential," *Journal of Food Biochemistry* 48, no. 4 (2024): e14267, https://doi.org/10.1155/2024/3625267.

42. R. M. P. Gutiérrez, S. Mitchell, and R. V. Solis, "*Psidium guajava*: A Review of Its Traditional Uses, Phytochemistry and Pharmacology," *Journal of Ethnopharmacology* 117, no. 1 (2008): 1–27, https://doi.org/10.1016/j.jep.2008.01.025.

43. E. M. El-Deeb, H. E. Elsayed, H. B. Ateya, et al., "Phenolic Profiling And Bioactivity Assessment of *In Vitro* Propagated *Psidium cattleianum* Sabine: A Promising Study," *Heliyon* 10, no. 8 (2024): e29379, https://doi.org/10.1016/j.heliyon.2024.e29379.

44. C. S. Pereira, S. Thompson, and B. L. Xavier, "AI-2-Mediated Signalling in Bacteria: A Universal Language and Its Implications in Virulence and Interspecies Communication," *FEMS Microbiology Reviews* 37, no. 2 (2013): 156–181, https://doi.org/10.1111/j.1574-6976.2012.00345.x.

45. R. D. Hernandez, F. A. F. Genio, J. R. Casanova, et al., "Antiproliferative Activities and SwissADME Predictions of Physicochemical Properties of Carbonyl Group-Modified Rotenone Analogues," *ChemistryOpen* 13, no. 1 (2024): e202300087, https://doi.org/10.1002/open.202300087.

Supporting Information

Additional supporting information can be found online in the Supporting Information section.

Supporting File: ansa70077-sup-0001-SuppMat.pdf.